

STUDY OF THE DISTRIBUTION OF SOLIDS IN A COUNTERFLOW BAFFLED GAS-SUSPENSION CHAMBER BY THE BETA-RAY METHOD

L. M. Belyi, Z. R. Gorbis, and I. K. Shumakov

Inzhenerno-Fizicheskii Zhurnal, Vol. 15, No. 1, pp. 66-72, 1968

UDC 536.27

The distribution of solids over the height and cross section of a counterflow baffled gas-suspension chamber has been investigated by the beta-ray method. The particles are decelerated by introducing spiral mesh baffles.

Starting from the penetrating power of the radiation and the expected concentration of solids in the apparatus, as the radiation source we chose a BI-1 standard beta emitter (a strontium 90 + yttrium 90 preparation with maximum energy  $E_{\max} = 2.18$  MeV).

When  $\beta$ -radiation passes through a layer of matter, the change in the intensity of the radiation can be approximately (up to about  $x = 7/\rho$ ) described by the equation

$$N = N_0 e^{-M_1 x} \tag{1}$$

It has been experimentally established [1] that the ratio  $M_1/\rho$  depends only slightly on the chemical composition of the absorber. This ratio is called the mass absorption coefficient  $M_m$  and is determined from the formula  $M_m = 22E_{\max}^{-1.33}$ .

In the case of quartz sand the  $M_m$  for the beta emission of  $Sr^{90} + Y^{90}$  is equal to  $M_m = 22 \cdot 2.18^{-1.33} = 7.8$   $cm^2/g$ , whence  $M_1 = M_m \rho = 7.8 \cdot 1.6 = 12.5$   $cm^{-1}$ , where  $\rho = 1.6$   $g/cm^3$  is the bulk density of the investigated fraction.

Knowing the linear attenuation factor  $M_1$ , and the beta particle flux in the absence of an absorber  $N_0$  and after passage through the absorber  $N$ , we can determine from (1) the thickness of the irradiated layer

and then the linear concentration:

$$x = \frac{\ln N_0 - \ln N}{M_1} \tag{2}$$

To check (2) we performed calibration tests. We first measured the intensity of the radiation  $N_0$  passing through the empty channel and then the intensity of the radiation passing through a layer of sand of varying thickness. During each experiment (duration 1 min) we measured the background  $N_b$ . In accordance with Fig. 1, the discrepancies between the experimental and calculated data do not exceed 3% at  $x \leq 0.3$  cm.

The experimental apparatus consisted of a "baffled gas-suspension" rig, a type PP-8 radiometer, and BI-1  $\beta$ -radiation source. The "baffled gas-suspension" rig is described in [2].

The air velocity in the chamber was varied from 0 to 1.3 m/sec. The granular charge, whose flow rate was varied from 500 to 1240 kg/hr, entered the chamber through a perforated sliding plate in a direction opposite to that of the air stream. In addition to estimating the distribution of solids over the height and cross section of the chamber in various operating regimes with and without (free suspension) various spiral baffles, we studied the effects of these factors on the aerodynamic drag  $\Delta p$  of the chamber.

The experimental data obtained in [2] enabled us to establish the optimal variants and geometric characteristics of the spiral baffles used in that research. For the mechanical deceleration of the falling particles

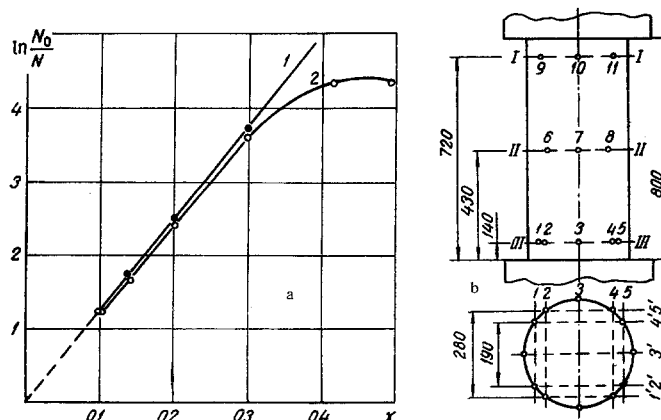


Fig. 1. Calibration curves (a: 1—calculated, 2—experimental; x in cm) and distribution of measuring points (b).

Table 1

Geometric Characteristics of the Spiral Mesh Baffles

Type of mesh opening	$F_{uc}$	$d_e$	Pitch of spiral, mm	Angle of inclination $\alpha^\circ$	Number of turns $n$	$d_e/d_p$
Square (woven mesh)	0.66	2.2	150	8	5.33	3.66
Round (punched mesh)	0.327	5.0	150	8	5.33	8.33

we used the two spiral mesh baffles whose geometric characteristics are given in Table 1. As the granular charge we used fractionated quartz sand with  $d_p = 0.6$  mm.

The radiation source and the photomultiplier unit were placed in lead containers to reduce the background and diffuse radiation. In order to create a narrow beam, coaxial cylindrical channels (collimators) with openings 5 mm in diameter were formed in the lead containers. At the measuring points through openings 5 mm in diameter were formed coaxially with the emitter-receiver, which also improved the collimation of the beam. The roller stand of a GUP-type apparatus was used to stabilize the relative position of the collimator axes and for the displacement, relative to height and cross section, of the source-receiver system.

Irradiation was carried out between the turns of the spiral baffle in three cross sections along the height of the chamber and at 3–5 points in each section in two mutually perpendicular directions (Fig. 1b). At each point we measured the intensity of the radiation  $N_0$  in the empty chamber. Then we created the necessary counterflow gas-suspension regime and measured the intensity of the radiation  $N$  at the same point (not less than 4–5 times). From the calibration curve (Fig. 1a) we found the thickness of the irradiated layer  $x$  of solid component and from the ratio of the layer thickness to the cross section of the chamber at the given point we determined the linear particle concentration  $\beta'_l$ . We then constructed concentration distribution diagrams over the height and cross section of the chamber and by planimetry found the mean volume concentration  $\beta$ . For comparison, we also used the rapid cutoff method, which enabled us to determine the mean volume concentration  $\beta_0$ . For the purpose we installed cutoff valves at the chamber inlet and outlet.

The standard deviation of the number of registered particles can be estimated in accordance with [3]:  $G_T = 100/(N\tau)^{1/2}$ , where  $N$  is the counting rate, pps. In our experiments  $N\tau$  was on the order of 7000 pulses, whence  $G_T = \pm 1.2\%$ . During the motion of the disperse flow  $G_T$  increased and at  $\beta = 38 \cdot 10^{-4}$  reached  $\pm 3.33\%$ . Altogether we performed 24 series of experiments with a total of 336 measured points.

The curves in Fig. 2a represent the distribution of the linear concentration  $\beta_l$  over the height and cross section of the chamber for the free and baffled suspen-

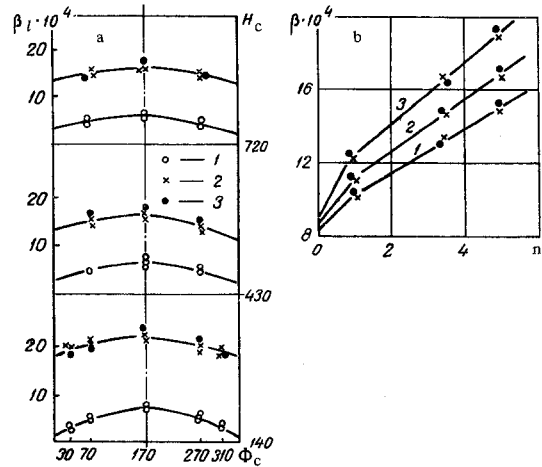


Fig. 2. Diagrams showing the distribution of solids over the cross section (a) and height of the chamber as a function of the number of turns  $n$  of the spiral baffle and  $Re$  (b) ( $\beta_l$ ,  $\beta$  in  $m^3/m^3$ ): a) 1—free suspension; 2—woven mesh  $d_e/d_p = 3.66$ ; 3—punched mesh  $d_e/d_p = 8.33$ ; b) 1— $Re = 0$ ; 2— $Re = 2.03 \cdot 10^3$ ; 3— $Re = 2.86 \cdot 10^3$ .

sion, other things being equal. Varying the parameters over the intervals  $Re = 0-2.86 \cdot 10^3$  and  $\mu = 1.24-2.91$   $kg \cdot hr/kg \cdot hr$  had no effect on the nature of the distribution. In this case mechanical deceleration causes an increase in the solids concentration by a factor of 2–3. Since the particles now fall by rolling along the turns of the mesh and spilling through, the increase in dwell time and hence the increase in concentration are perfectly natural. Aerodynamic deceleration of the falling particles by the air counterflow increased the solids concentration by only 20% as compared with the case  $v_a = 0$ . A further increase in air velocity above 1.9 m/sec led to entrainment of the particles. For the free suspension the mean concentration over the cross section did not vary along the height of the chamber, which indicates the rapid onset of uniform motion in a counterflow [4]. In the baffled suspension, however, the concentration did not remain constant with respect to height, but the nature of the particle distribution over the cross section was the same as in the free suspension—the curves are almost equidistant with a maximum along the chamber axis and a symmetrical variation of concentration toward the periphery. However, in accordance with Table 2, the degree of

Table 2

## Degree of Nonuniformity of Particle Distribution Over Chamber

Re · 10 <sup>4</sup>	Free suspension			Woven mesh $d_e/d_p = 3.66$			Punched mesh $d_e/d_p = 8.33$		
	I	II	III	I	II	III	I	II	III
0	0.863	0.832	0.825	0.805	0.814	0.740	0.787	0.750	0.633
2.03	0.832	0.845	0.885	0.803	0.770	0.840	0.610	0.650	0.600
2.86	0.880	0.840	0.808	0.814	0.722	0.785	0.620	0.740	0.690

Remark. I, II, and III denote the chamber cross sections.

Table 3

Concentration Data Obtained by the Cutoff Method and the  $\beta$ -Ray Method

Particle flow rate $G_p$ , kg/hr	Air flow rate $G_a$ , kg/hr	$\mu = \frac{G_p}{G_a}$ kg/hr	Mean volume concentration $\beta \cdot 10^4$ , m <sup>3</sup> /m <sup>3</sup> :					
			Cutoff method			$\beta$ -ray method		
			I	II	III	I	II	III
550	0	—	5.8	12.6	12.8	5.75	11.8	12.0
1026	0	—	9.6	22.3	22.0	9.64	20.6	20.2
608	374	1.64	6.53	15.6	14.4	6.35	14.5	14.0
1090	374	2.91	12.0	27.8	28.3	12.0	25.0	25.7
663	526	1.26	9.20	22.5	24.0	8.90	21.0	22.0
1233	526	2.34	14.4	32.2	32.0	14.0	29.8	30.0

Remark. I—free suspension, II and III—baffled suspension, mesh  $d_e/d_p$  respectively equal to 3.66 and 8.33.

nonuniformity of particle distribution over the cross section, estimated from the ratio of the maximum to the mean value of  $\beta_I$ , is different. For flow deceleration using a punched mesh the nonuniformity is much greater than for a free suspension, and for deceleration using a woven mesh approximately the same. It is important to note the effect of the number of baffles on the variation of the mean concentration, which could be estimated thanks to the use of the  $\beta$ -ray method. In accordance with Fig. 2b, each successive turn of the spiral baffle increases the concentration. Beyond the first turn the dependence is linear; the slope depends on the Re number and also on the geometry of the mesh. The use of a punched mesh with  $F_{uc} = 0.327$  and  $d_e/d_p = 8.33$  gives the same deceleration effect as a woven mesh with  $F_{uc} = 0.66$  and  $d_e/d_p = 3.66$  (Fig. 2a). This result can be attributed to the opposite effect of  $F_{uc}$  and  $d_e/d_p$  on the increase in the dwell time of the mass of particles in the air flow. However, woven mesh is to be preferred, since punched mesh causes a deterioration in the uniformity of distribution of the charge and creates a greater resistance to the passage of air. The results obtained by  $\beta$ -ray irradiation in mutually perpendicular directions showed that the concentration distribution is symmetrical.

The transparent chamber also enabled us to make visual observations. The formation on the mesh of an undeveloped fluidized moving bed distributed over the turns of the spiral is typical. The motion of the particles alternates with spilling through the mesh openings onto the lower turns of the spiral. The thickness of the fluidized bed fluctuates with the particle flow rate, the air velocity in the chamber, and the type of mesh. The maximum thickness reached about 25–30  $d_p$  on a mesh with  $d_e/d_p = 8.33$ .

The results of determining the mean volume concentration  $\beta$  over the chamber, obtained by the cutoff method and the  $\beta$ -ray method, are summarized in Table 3 (the discrepancies do not exceed 10%). The values of  $\beta$  obtained by the  $\beta$ -ray method give results that are somewhat too low, since the increase in concentration due to fluidization of the particles on the turns of the mesh was not taken fully into account. Determination of  $\beta$  for a nonuniform supply of solid phase over the chamber cross section (the particles were introduced centrally through two openings 25 mm in diameter) revealed the equalizing effect of the spiral baffle. However, at  $n = 5.33$  it was not possible to achieve total uniformity of distribution.

The pressure loss  $\Delta p$  of the air flow in the chamber for a free and a baffled gas suspension was determined using static taps in the upper and lower parts of the chamber and an MMN micromanometer graduated in 0.2 kg/m<sup>2</sup>. According to Fig. 3, the use of mesh baffles causes an increase in the resistance to the passage of air, which is attributable to the increased blocking of the chamber and a local increase in velocity. The resistance of the baffles is a function of the number of turns and the useful cross section of the mesh. The ratio  $d_e/d_p$  characterizes the degree to which the passage of particles through the mesh openings is restricted and the extent to which the mesh blocks the passage of air. The first factor increases the mechanical deceleration, while the second creates the conditions for the nonuniform distribution of air over the chamber cross section leading to an increase in the mechanical deceleration effect. As the flow-rate concentration  $\mu$  increases, so does the aerodynamic drag of the chamber, which is natural since the number of particles simultaneously in the chamber increases. This relation is shown in Fig. 3 as a continuous line.

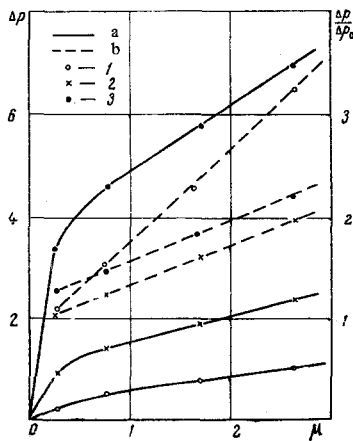


Fig. 3. Pressure loss ( $\text{kg}/\text{m}^2$ ) as a function of concentration ( $\text{kg}/\text{hr}/\text{kg}/\text{hr}$ ) (a— $\Delta p/\Delta p_0$ ): 1) free suspension; 2) woven mesh; 3) punched mesh.

However, the relative pressure loss  $\Delta p/\Delta p_0$  ( $\Delta p_0$  is the resistance of the chamber without a charge) is less than in the free suspension.

The possibilities of increasing the efficiency of counterflow disperse systems using spiral mesh baffles are not exhausted by the data presented. Thus, in [2] in the rolling-spilling regime at  $d_e/d_p = 1.1$  and  $F_{uc} = 0.327$  the residence time of the particles increased approximately by a factor of 18, which is chiefly attributable to the increase in the period of rolling along the turns of the spiral. As a result of the improved aerodynamics in a chamber with a mesh opening diameter  $d_0 = 2.8$  mm, i. e.,  $d_e/d_p = 4.66$ ,  $F_{uc} = 28\%$ , it proved possible to achieve an increase in the particle residence time by a factor of approximately 9.

The use of the  $\beta$ -ray method to estimate the variation of the true concentrations over the cross section

and height of a counterflow chamber enabled us to detect an increase in true concentration along the path of the particles and a fairly uniform distribution of the particles over the cross section, and to confirm the desirability of using mesh with a small  $d_e/d_p$  ratio and a large useful cross section. The latter also makes possible a significant reduction in aerodynamic drag (Fig. 3).

For a complete evaluation of the proposed method of mechanical deceleration it will subsequently be necessary to obtain data on the heat transfer in such systems.

#### NOTATION

$N$  is the beta flux;  $\mu_{l,m}$  is the linear mass  $\beta$ -flux attenuation factor;  $x$  is the thickness of the absorber;  $\rho$  is the density;  $d_p$  is the particle size;  $d_e$  is the equivalent diameter of the openings;  $v_a$  is the air velocity;  $v_c$  is the critical velocity;  $F_{uc}$  is the useful cross section;  $\beta$  is the volume concentration;  $\Delta p$  is the pressure drop;  $\mu$  is the flow-rate mass concentration;  $H_c$  is the height of the chamber.

#### REFERENCES

1. N. N. Shumilovskii, Yu. P. Betin, B. N. Verkhovskii, et al., Radioisotope and X-Ray Spectral Methods [in Russian], Energiya, 1965.
2. Z. R. Gorbis, L. M. Belyi, and I. K. Shumakov, IFZh [Journal of Engineering Physics], **11**, no. 1, 1966.
3. I. V. Estulin, Radioactive Radiations [in Russian], Gos. izd. fiziko-matematicheskoi literatury, 1962.
4. Z. R. Gorbis, Heat Transfer of Disperse Through Flows [in Russian], Energiya, 1964.

22 May 1967

Lomonosov Technological  
Institute, Odessa